The Journal of Chemical Physics

RESEARCH ARTICLE | JANUARY 03 2023

Inducing SERS activity at graphitic carbon using graphene-covered Ag nanoparticle substrates: Spectroelectrochemical analysis of a redox-active adsorbed anthraquinone

Kendrich O. Hatfield ; Seth T. Putnam ; Joaquín Rodríguez-López

J. Chem. Phys. 158, 014701 (2023)
https://doi.org/10.1063/5.0130876

AIP Publishing

The Journal of Chemical Physics ARTICLE scitation.org/journal/jcp

Inducing SERS activity at graphitic carbon using graphene-covered Ag nanoparticle substrates: Spectroelectrochemical analysis of a redox-active adsorbed anthraquinone

Cite as: J. Chem. Phys. 158, 014701 (2023); doi: 10.1063/5.0130876
Submitted: 15 October 2022 • Accepted: 7 December 2022 •
Published Online: 3 January 2023

Kendrich O. Hatfield, Seth T. Putnam, and Joaquín Rodríguez-López[a)]

AFFILIATIONS

Department of Chemistry, University of Illinois at Urbana-Champaign, Urbana, Illinois 61801, USA

Note: This paper is part of the JCP Special Topic on *In situ* and *Operando* Characterization.
[a)]**Author to whom correspondence should be addressed:** joaquinr@illinois.edu

ABSTRACT

Graphitic carbon electrodes are central to many electrochemical energy storage and conversion technologies. Probing the behavior of molecular species at the electrochemical interfaces they form is paramount to understanding redox reaction mechanisms. Combining surface-enhanced Raman scattering (SERS) with electrochemical methods offers a powerful way to explore such mechanisms, but carbon itself is not a SERS activating substrate. Here, we report on a hybrid substrate consisting of single- or few-layer graphene sheets deposited over immobilized silver nanoparticles, which allows for simultaneous SERS and electrochemical investigation. To demonstrate the viability of our substrate, we adsorbed anthraquinone-2,6-disulfonate to graphene and studied its redox response simultaneously using SERS and cyclic voltammetry in acidic solutions. We identified spectral changes consistent with the reversible redox of the quinone/hydroquinone pair. The SERS intensities on bare silver and hybrid substrates were of the same order of magnitude, while no discernible signals were observed over bare graphene, confirming the SERS effect on adsorbed molecules. This work provides new prospects for exploring and understanding electrochemical processes *in situ* at graphitic carbon electrodes.

INTRODUCTION

Graphitic carbon electrodes are integral to many electrochemical energy technologies involving electrocatalysis and energy storage.[1–4] Beyond acting as supports for materials and catalysts, the role of the carbon chemistry is decisive in energy storage devices such as lithium-ion batteries,[5] redox-flow batteries,[6] and supercapacitors,[7] providing a strong incentive for thoroughly understanding their electrochemical behavior. Electrochemical methods can characterize electron transfer kinetics and mechanisms involving molecular species at these electrodes.[8,9] However, these techniques lack the ability to identify surface speciation and molecular structural changes occurring during redox reactions. To address these shortcomings, the coupling of methods such as nuclear magnetic resonance (NMR),[10,11] UV–vis,[12,13] and IR spectroscopies[13] with electrochemistry enables the correlation of redox reactivity with the speciation at the surface of the electrode and near-interface region. In particular, Raman spectroscopy,[14] which is based on the inelastic scattering of photons interacting with the analyte's vibrational modes, stands out for its ability to track chemical and structural changes in electrodes and molecules with micrometer-scale spatial resolution. Furthermore, the straightforward implementation of Raman spectroscopy makes it ideal for *in situ* and *operando* electrochemical characterization. However, the inherent low sensitivity of Raman spectroscopy necessitates enhancement mechanisms such as those found in tip-enhanced Raman spectroscopy,[15] resonance Raman spectroscopy,[16] and surface-enhanced Raman scattering (SERS)[17] to effectively probe electrode surfaces. This is because the electrochemical interface consists of a thin, nanometer-scale region, which limits the number of scattering species of interest. Once more, SERS is particularly useful, due to its relative ease of setup and wide applicability in various electrolytes and analytes.

SERS uses a plasmonic substrate (most often Au- or Ag-based) to drastically improve the signal obtained from species directly adjacent to the substrate surface.[18] SERS enhancement arises from two effects: chemical and electromagnetic enhancements. If the incoming laser wavelength overlaps with the plasmon resonance band of the substrate, electrons within the substrate are excited into an oscillating wave called a plasmon. Chemical enhancement involves the transfer of charge density from the surface plasmons to the analyte molecule, inducing changes in its polarizability. This is a very short-range effect, requiring the analyte to be in near contact with the surface. On the other hand, electromagnetic enhancement arises from the drastic increase of the electromagnetic field near the plasmons and can extend up to ~10 nm away from the surface.[18,19] The combined SERS effect has been extensively leveraged to probe electrochemical systems,[17] though the need for a plasmonic substrate has set strict requirements for amenable electrode systems. Carbon itself can be effectively studied with Raman spectroscopy,[20] but it is not plasmonic, making the detection of adsorbed species and transient surface intermediates impractical at unmodified carbon electrodes.

Considering that SERS is overall a very short-range phenomenon,[21] graphene's atomic-scale thickness is a strong advantage, enabling SERS activity on carbon with underlying nanoparticles.[22] In this study, we demonstrate a hybrid nanoparticle–graphene electrode to perform electrochemical SERS on a carbon electrode. Transferring multi-layer graphene (MLG) or single-layer graphene (SLG) onto fluorine-doped tin oxide (FTO, a transparent semiconductor) coated with silver nanoparticles (AgNPs) yields a substrate with flexible applications for electrochemical SERS (Fig. 1), analogous to plasmonic nanoparticles coated in silica or alumina used for shell-isolated nanoparticle-enhanced Raman spectroscopy (SHINERS).[23]

Anthraquinone-based electrochemistry is an excellent first candidate to study our substrate. Anthraquinone and its derivatives are known to adsorb to sp^2 hybridized carbons,[24] and their redox properties display a variety of applications, ranging from redox flow batteries[25] to commercial hydrogen peroxide production.[26] Here, we use disodium anthraquinone-2,6-disulfonate (AQDS) because of previous studies showing its adsorptive electrochemical properties.[27] AQDS can undergo a proton-coupled two-electron reduction in aqueous systems (Fig. 1),[28] in which the quinone groups are transformed into hydroquinone groups, significantly impacting the Raman spectrum. In this study, we adsorb AQDS to a hybrid graphene–silver nanoparticle substrate, where the metal component is buried below the graphitic carbon, to observe SERS spectra during electrochemical cycling. This substrate design should open avenues for more complete insight into a variety of important redox processes occurring on carbon electrodes for *in situ* and *operando* characterization of energy conversion and storage technologies.

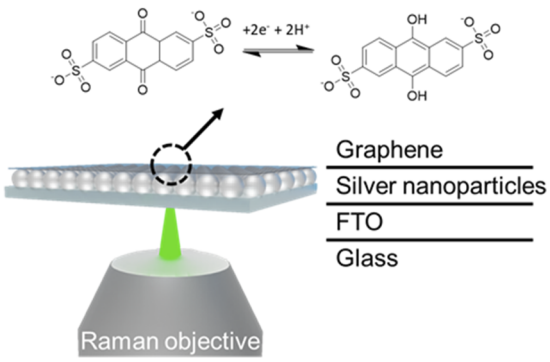

FIG. 1. Schematic of electrochemical SERS of the proton-coupled AQDS redox reaction on a hybrid nanoparticle–graphene electrode. FTO stands for fluorine-doped tin oxide electrode on a glass cover slip. AQDS is adsorbed onto the electrode.

EXPERIMENTAL

Materials

Silver nanoparticles with an average diameter of 65 ± 12 nm were synthesized in the same manner as in previous studies.[29] Briefly, 100 ml water and 18.0 mg $AgNO_3$ (99%, Sigma-Aldrich) were combined in a 125 ml Erlenmeyer flask and brought to a rolling boil under stirring at 600 rpm. 4 ml of 5% m/v sodium citrate dihydrate (Fisher Scientific) was then added, and the solution was stirred at a light boil for 60 min, during which the solution turned an opaque yellow–green color. The heat was then shut off and the solution cooled to room temperature, while stirring on the hot plate 60 min. The resulting solution was centrifuged at 5000 relative centrifugal field for 15 min, then the supernatant was discarded, and the pellet was diluted to 10 ml with water. This method yielded 65 ± 12 nm particles.[29] Ultrapure water from a Millipore Synergy purifier was used for all solutions. Copper etchant type CE-100 (Transene), ethylenediaminetetraacetic acid disodium dehydrate salt (EDTA, VWR), (3-aminopropyl)trimethoxysilane (APTMS, 97%, Sigma-Aldrich), poly(bisphenol A carbonate) (Aldrich), Chloroform (Macron), sodium chloride (Sigma-Aldrich), hydrogen peroxide (30% in water, J. T. Baker), sulfuric acid (95%, Fisher Chemicals, used for Piranha cleaning solution), sulfuric acid for trace metal analysis (Fisher Chemicals, used for all electrochemistry and AQDS adsorption), perchloric acid (70%, Veritas), isopropanol (Honeywell), and disodium anthraquinone-2,6-disulfonate (AQDS, ChemCruz) were used as received for all solutions and cleaning processes. Multi-layer graphene (MLG) was grown on cleaned copper foil at 1000 °C for 5 min under a constant flow of 30 SCCM of hydrogen gas and 10 SCCM of methane gas;[30] SLG on copper foil was purchased from Grolltex. MLG was characterized via optical transmission microscopy and found to be 10–15 layers thick across most of the film, with thinner spots (1–5 layers) present as well.

AgNP coating method

All fluorine-doped tin oxide (FTO, Delta Technologies, 5–15 Ω/sq) slides were cleaned in Piranha solution (3:1 mixture of concentrated H_2SO_4 and 30% H_2O_2) for ~30 min. *Safety note: Piranha solution is highly oxidizing and potentially explosively reactive with organic compounds including solvents.* The slides were then sonicated 15 min three times in ultrapure water, followed by three times in isopropanol. The clean FTO slides were dried with ultra-high purity Ar gas (Airgas) and soaked 30 min in 5% APTMS in ethanol. They were then rinsed thoroughly with ethanol and dried with Ar gas before dropcasting enough AgNP solution to cover the

entire surface. The slides were left with the AgNP solution overnight in a 100% humidity box to allow nanoparticle film formation.

Graphene transfer

MLG was transferred directly onto both plain and AgNP-coated FTO via wet-transfer. First, 3% poly(bisphenol A carbonate) was spincoated (10 s at 1000 rpm, followed by 30 s at 3000 rpm) onto the MLG on copper to support the graphene. The exposed side of the graphene was cleaned for 5 min in a Harrick-Plasma PDC-001-HP plasma cleaner (atmospheric air) on the highest energy setting. The copper support was removed by floating for 20 min on a copper etchant solution. A glass slide was then used to transfer the graphene to ultrapure water four subsequent times before transferring to a 0.1M EDTA solution, where it was soaked for 2 h. The graphene was then transferred four times to ultrapure water before transferring onto the plain FTO or FTO/AgNP substrates. The MLG-covered substrates were dried under vacuum overnight and then soaked at least 6 h in chloroform, followed by copious rinsing in acetone and isopropyl alcohol to remove the poly(bisphenol A carbonate) layer. SLG substrates were transferred in the same manner.

Electrochemical SERS experiment

MLG-covered substrates were soaked in a 5 mM AQDS solution with trace metal analysis grade 0.1M H_2SO_4 for 2 h to adsorb anthraquinone before being mounted onto the electrochemical cell. The cell was filled with an aqueous 0.1M H_2SO_4 solution, covered with parafilm, and purged with argon gas to remove atmospheric oxygen. A 532 nm laser (Melles Griot, 200 mW), with no optical density filter, was aligned to the substrate surface through a 50× long-distance working objective (Olympus; NA, 0.5). SERS spectra were recorded with an Ocean Optics QE Pro spectrometer (2 s integration time unless otherwise noted) while performing voltammetry with a CHI 920D potentiostat, with a platinum wire for a counter electrode and an Ag/AgCl reference electrode connected to the cell via an agar/0.1M $NaClO_4$ salt bridge. All potentials in this work are referenced with respect to the latter electrode.

Equipment

SERS instrumentation was identical to that used in previous studies,[29] and a Nanophoton Raman 11 microscope with a 532 nm laser was used in addition to further characterize substrates. Note that minor wavenumber discrepancies appear between this spectrometer and the QE Pro, likely due to differences in calibration and resolution. A JEOL 7000F scanning electron microscope with a Thermo Electron energy-dispersive x-ray spectrometer (EDS) was used to image the AgNP-coated substrates.

RESULTS AND DISCUSSION

MLG/AgNP SERS

To fabricate the SERS-active graphene substrates, we first grafted AgNPs onto cleaned FTO via APTMS functionalization, and then transferred MLG onto the bare nanoparticles. This strategy provides an optically transparent and electrically conductive contact to the graphene. Figure 2(a) shows an SEM micrograph of bare and

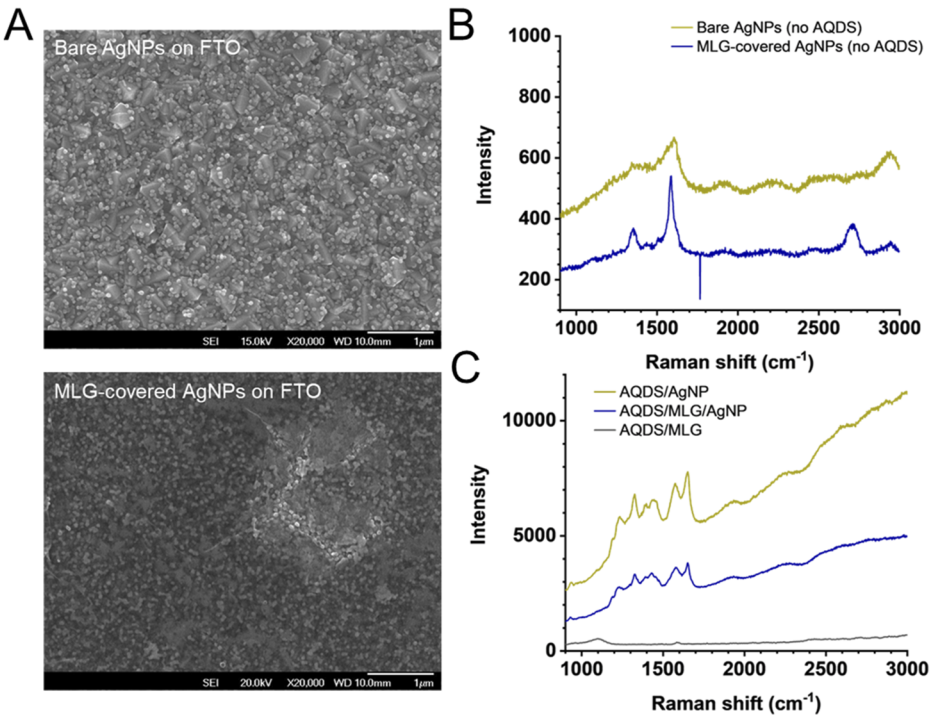

FIG. 2. MLG/AgNP substrate characterization. (a) SEM images of bare and MLG-covered AgNPs on FTO. (b) Raman spectra of plain MLG/AgNP and bare AgNPs. (c) SERS spectra of adsorbed AQDS on bare and MLG-covered AgNPs, with comparison to bare MLG electrode exposed to AQDS.

MLG-covered AgNPs deposited on FTO, suggesting that the underlying morphology of the electrode does not change significantly due to graphene transfer, although differences in the SEM contrast indicate that the sample conductivity is affected due to the placing of the graphene sheet.

First, we focus on the SERS response of AQDS over MLG/AgNP electrodes and their comparison to MLG and AgNP electrodes. The SERS traces in Fig. 2(b) show the Raman spectra of a dry MLG/AgNP substrate compared to plain AgNPs, with the former displaying the expected D, G, and 2D peaks of graphene at 1350, 1594, and 2692 cm^{-1}, respectively.[20] Figure 2(c) shows MLG, MLG/AgNP, and AgNP electrodes, which were soaked for 2 min in 5 mM AQDS with 0.1M $HClO_4$, subsequently rinsed, and allowed to dry. After exposure to the AQDS solution, molecular adsorption revealed a greatly increased Raman scattering, by about one order of magnitude difference, when compared to the bare MLG/AgNP and AgNP electrodes shown in Fig. 2(b). This adsorption is evidenced by new bands that appear in both cases, overwhelming those intrinsic to the MLG layer. In addition, a bare MLG electrode on which AQDS adsorption was carried out, displayed no such bands, thus allowing us to confidently conclude a SERS effect on the adsorbed AQDS on MLG/AgNP and AgNP. We assigned the SERS bands on AgNP and MLG/AgNP to the asymmetric SO_3^- stretching (1194 cm^{-1}), C=C ring stretching (1328, 1390, and 1582 cm^{-1}), and C=O stretching (1650 cm^{-1}) vibrational modes.[31,32] The peak intensities of AQDS on the AgNP electrode are about three times as intense as those on the MLG/AgNP electrode, implying some attenuation of the SERS effect in the latter. Considering the two SERS enhancement effects, it is probable that the shorter-range chemical enhancement mechanism

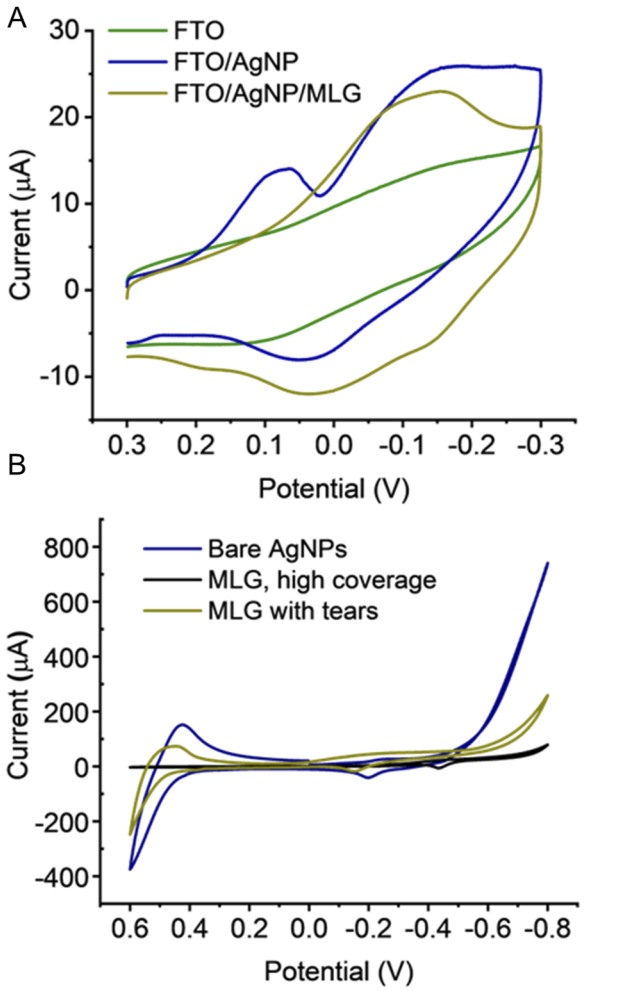

FIG. 3. Substrate electrochemistry. (a) Cyclic voltammograms (100 mV/s) of adsorbed AQDS on plain FTO, FTO with AgNPs, and FTO/AgNP/MLG in 0.1M H_2SO_4. (b) Cyclic voltammograms (100 mV/s) of bare AgNPs and MLG-covered AgNPs, including MLG with high coverage and MLG with significant tears/pinholes, in 0.1M H_2SO_4.

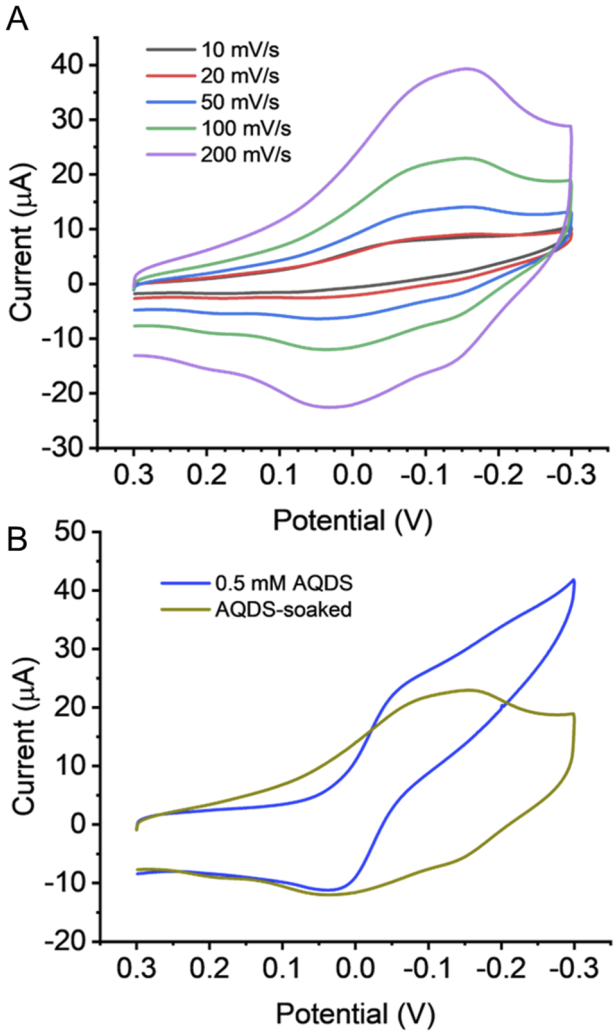

FIG. 4. AQDS voltammetry on MLG/AgNP substrates. (a) Cyclic voltammograms at various scan rates in 0.1M H_2SO_4 on an MLG/AgNP substrate soaked 2 h in 5 mM AQDS with 0.1M H_2SO_4. (b) 100 mV/s cyclic voltammograms of plain MLG/AgNP substrates in 0.5 mM AQDS (blue) alongside MLG/AgNP soaked 2 h in 5 mM AQDS with 0.1M H_2SO_4. All solutions use 0.1M H_2SO_4 as electrolyte.

is decreased by the distance introduced by the MLG sheet that stands between the AgNPs and the AQDS adsorbed layer. However, since electromagnetic enhancement is often the dominant SERS mechanism,[18] our results showing only mild attenuation at the MLG covered substrates are reasonable.

To demonstrate the adsorption electrochemistry of AQDS on these substrates, we soaked plain FTO, FTO/AgNP, and FTO/AgNP/MLG substrates for 2 h in 5 mM AQDS with 0.1M H_2SO_4 and recorded cyclic voltammograms at 100 mV/s [Fig. 3(a)] in 0.1M H_2SO_4. For each substrate, we observe a reversible wave centered around −0.05 V that we attribute to AQDS. On plain FTO, this adsorption peak (if any) is weak. We also observe a peak on the FTO/AgNP around 0.1 V, which we attribute to AQDS or some interaction of AQDS with Ag oxides, as it is not present in the voltammetry of FTO/AgNP in the absence of AQDS (see below). To show the added electrochemical stabilization that MLG provides to the FTO/AgNP substrate, we performed cyclic voltammograms with wider potential windows on FTO/AgNP and FTO/AgNP/MLG in 0.1M H_2SO_4 [Fig. 3(b)]. On the bare AgNPs, we observe Ag oxidation beginning near 0.4 V, with a clear re-reduction peak upon the negative sweep. We did not observe this on a well-covered FTO/AgNP/MLG sample, though we saw that samples with tears and pinholes do allow some Ag oxidation. Also, at −0.8 V, we observe hydrogen evolution reaction (HER) currents nearing 800 μA at −0.8 V on the bare AgNPs, while the well covered MLG sample presented currents of <100 μA. When the MLG cover was defective, the current was in-between these values, at ~200 μA. The results with MLG cover point to a potential window-broadening effect of the MLG via HER suppression. These results encourage the optimization of graphene coverage and quality if higher stability with electrode bias is desired.

We now evaluate the SERS performance of adsorbed AQDS on MLG/AgNP electrodes under electrochemical cycling. To test the SERS-electrochemistry of AQDS on these substrates under several conditions, we soaked MLG/AgNP electrodes for 2 h in 5 mM AQDS with 0.1M $HClO_4$, 1M $HClO_4$, or 0.1M H_2SO_4 before rinsing with water and mounting onto an electrochemical cell. We then filled the cell with the respective acid electrolyte, covered with parafilm, and purged with Ar gas. Cyclic voltammograms at different scan rates in 0.1M H_2SO_4 are shown in Fig. 4(a), which displays typical signs of molecular adsorption—first, because the AQDS redox is present even in the absence of AQDS in solution, and second, because the voltammetric peak increases in intensity with scan rate in a linear fashion.[33] Considering an electrochemically active area of 0.3 cm^2, an integrated forward peak yielding ~10 μC, and number of electrons as 2, we can estimate the molecular surface coverage as 1.7×10^{-10} mol/cm^2, very close to that of a monolayer of anthraquinone-2-carboxylic acid on gold measured by Han *et al.* (1.8×10^{-10} mol/cm^2).[34] Given the structural heterogeneity of these substrates, which may lead to many distinct interactions with the adsorbed AQDS molecules, it is not surprising to observe a broadened voltammogram with several features in the current profile. This voltammogram also shows the impact of traces of O_2 in the cell, which largely mask the chemically reversible redox wave of AQDS at lower scan rates. At faster scan rates, the AQDS redox is more clear, since the voltammetric peak current of an adsorbed redox species depends linearly on the scan rate, in contrast to redox species undergoing planar diffusion (i.e., O_2), which depend on the square root of

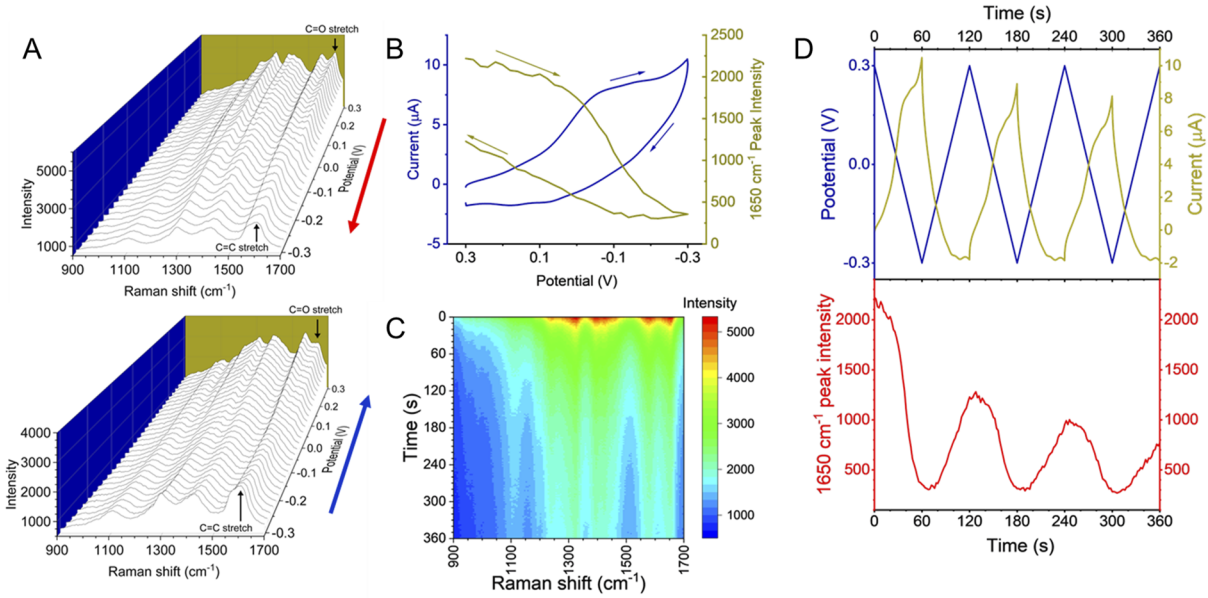

FIG. 5. Electrochemical SERS of MLG/AgNP soaked in 5 mM AQDS with 0.1M H_2SO_4. (a) SERS spectra taken during negative-going (top) and positive-going (bottom) cyclic voltammograms in 0.1M H_2SO_4. (b) Voltammetry of AQDS-soaked MLG/AgNP in 0.1M H_2SO_4, with the estimated 1650 cm^{-1} peak intensity. (c) SERS spectra taken over 6 min at a fresh spot on an AQDS-soaked MLG/AgNP substrate at open circuit. (d) Three voltammetry cycles with the estimated 1650 cm^{-1} peak plotted below, showing gradual decrease in SERS intensity over time.

the scan rate.[33] Figure 4(b) compares the 100 mV/s cyclic voltammograms of an AQDS-soaked MLG/AgNP electrode in 0.1M H_2SO_4 to a fresh one in a solution containing 0.5 mM AQDS in 0.1M H_2SO_4, demonstrating the matching redox potentials between adsorbed and solution AQDS. Overall, these tests showed the adsorption of AQDS unto the MLG/AgNP electrode and the ability to carry out cyclic voltammetry (CV) experiments in an AQDS-free electrolyte.

Electrochemical cycling gave rise to reversible SERS signatures consistent with the redox of the adsorbed AQDS. We measured Raman spectra during voltammetric cycling at 10 mV/s in 0.1M H_2SO_4, with an integration of 2s. Figure 5(a) shows the spectra measured during the first cycle split into the forward and reverse sweeps. The 1650 cm^{-1} peak corresponding to the C=O stretch disappeared upon AQDS reduction and reappeared upon reoxidation, indicating the reversibility of the quinone/hydroquinone forms presented in Fig. 1. Meanwhile, the peak at 1619 cm^{-1} assigned to the C=C stretching within the anthraquinone ring becomes prominent upon AQDS reduction, in agreement with results from Dai *et al.* on an anthraquinone derivative attached to gold via sulfur functionalization.[32] Estimating the height of the 1650 cm^{-1} peak by subtracting the average intensity between 1800 and 2000 cm^{-1} (used as proxy for background) from the absolute peak intensity shows the reversibility of the AQDS redox reaction, as shown in Fig. 5(b), overlaid with the voltammogram. However, this trace showed a decrease in the overall SERS intensity after the voltammogram. Moving the laser excitation to a new spot on the substrate and measuring the SERS spectra over 6 min with no applied potential shows that the intensity decrease occurs even without redox cycling [Fig. 5(c)]. Figure 5(d) shows the electrochemical SERS over three voltammetric cycles at one spot, again showing a decreasing SERS response over time. Figure 5(d) also shows that although not proportionate to the change in Raman intensity, the current intensity also decreased between the first and third cycles. These observations suggest that some of the signal degradation could be due to either AQDS desorption/degradation or some MLG/AgNP degradation promoted by laser exposure. To demonstrate that the response of our electrodes is not unique to the H_2SO_4 aqueous environment, we also probed experiments in $HClO_4$, obtaining similar SERS results as shown by the reversible traces in Figs. 6(a) and 6(b). Overall, the AQDS/MLG/AgNP assembly clearly shows reversible SERS signatures consistent with redox transformations.

To show the robustness of the MLG/AgNP substrates, we imaged them after electrochemical SERS experiments with SEM, including energy-dispersive x-ray spectroscopy (EDS). SEM micrographs of MLG-covered AgNPs with [Fig. 7(a)] and without [Fig. 7(b)] electrochemical SERS experimentation shows that ~70 nm particles are apparent across the FTO glass slide and that the morphology and appearance of the electrodes is similar. The EDS spectra at regions with high AgNP coverage show prominent peaks at 3.0 and 3.2 keV, representing the Lα and Lβ$_1$ lines for silver, respectively, while spectra at relatively bare regions show peaks mostly associated with tin and lighter elements [Fig. 7(c)]. Thus, the silver nanoparticles remain intact and bound to the FTO under the MLG after voltammetric cycling in acidic media, encountering only partial SERS effectiveness loss. These results indicate that these hybrid nanoparticle–graphene substrates are amenable to spectroelectrochemical studies of surface processes at carbon electrodes.

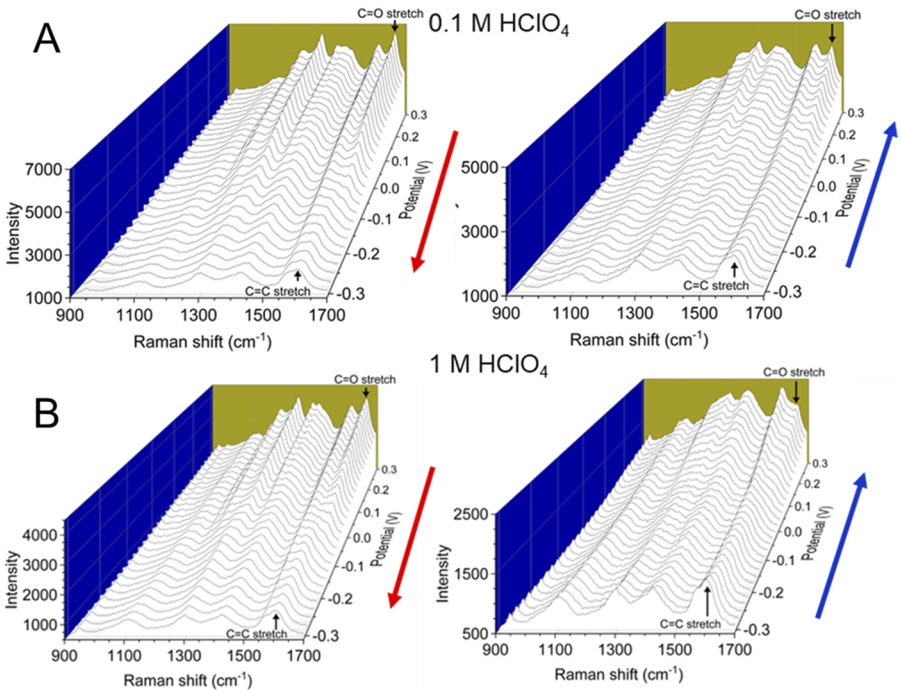

FIG. 6. Electrochemical SERS spectra taken during negative-going (left) and positive-going (right) cyclic voltammograms of MLG/AgNP substrates soaked in 5 mM AQDS with (a) 0.1M and (b) 1M $HClO_4$.

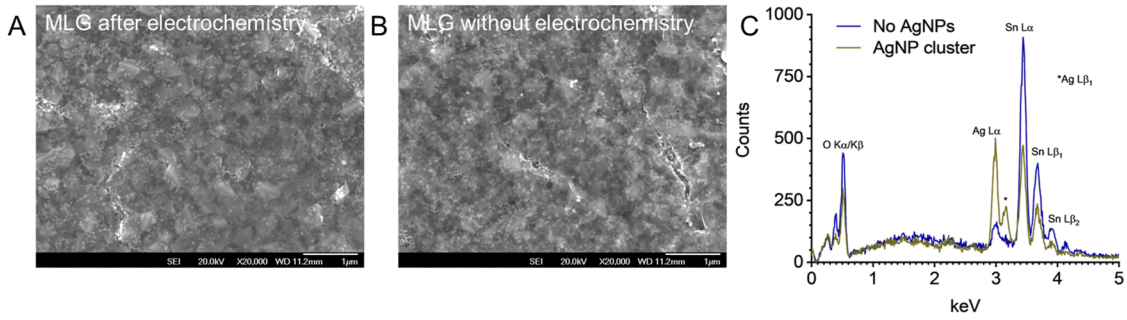

FIG. 7. SEM characterization of MLG/AgNP substrates before and after electrochemical SERS. SEM micrographs of MLG/AgNP both with (a) and without (b) electrochemical treatment are shown. (c) EDS spectra taken over AgNP-rich and AgNP-deficient regions of the substrate after electrochemical experiment.

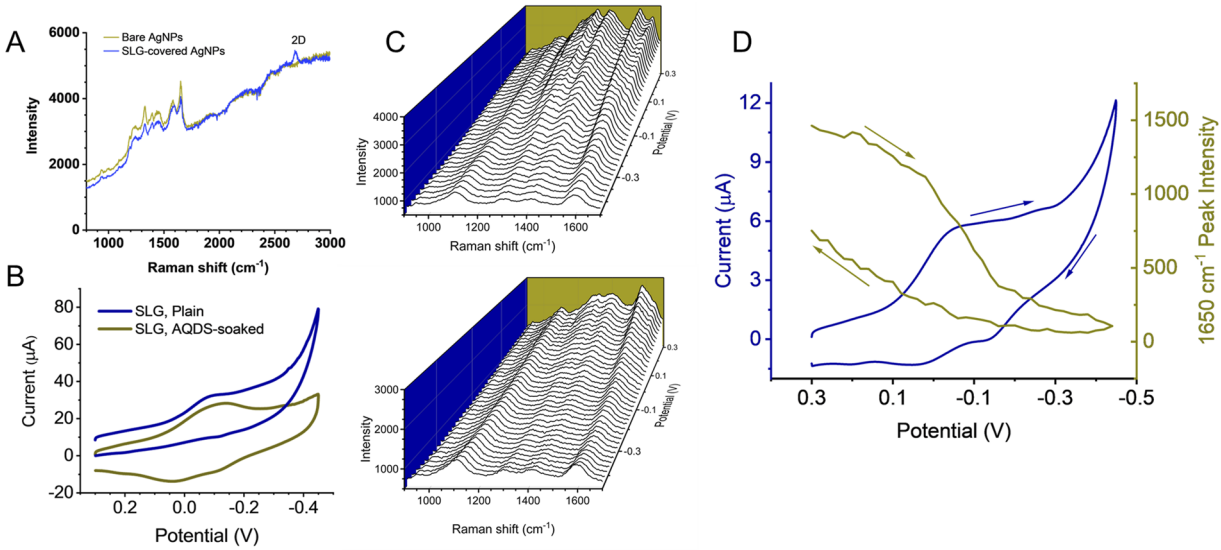

FIG. 8. Electrochemical SERS experimentation on SLG/AgNP substrates. (a) SERS spectra on bare and MLG-covered AgNPs soaked 2 min in 5 mM AQDS with 0.1M $HClO_4$. (b) Cyclic voltammograms at 100 mV/s of plain SLG/AgNP (blue), showing traces of oxygen, and SLG/AgNP soaked 2 h in 5 mM AgNP with 0.1M $HClO_4$. (c) SERS spectra recorded during cyclic voltammetry of AQDS-soaked SLG/AgNP (top: negative-going, bottom: positive-going). (d) Voltammetry of AQDS-soaked SLG/AgNP in 0.1M H_2SO_4, with the estimated 1650 cm^{-1} peak intensity.

SLG/AgNP results

To see the effect of graphene thickness on AQDS adsorption and SERS response, we transferred SLG onto AgNPs with the same wet transfer method as with MLG. We note that clean transfer of SLG onto these rough AgNP/FTO surfaces is less reproducible, likely due to the fragility of SLG compared to MLG, suggesting that alternative transfer methods could be explored for obtaining better SLG/AgNP substrates. Soaking the SLG/AgNP substrates for 2 min in 5 mM AQDS with 0.1M $HClO_4$ leads to nearly identical SERS spectra over bare and graphene-covered regions, as shown in Fig. 8(a), implying that the thinness of SLG does not attenuate the SERS enhancement of the AQDS much, if at all.

AQDS also showed reversible electrochemistry and SERS at SLG. Soaking an SLG/AgNP substrate in 5 mM AQDS with 0.1M $HClO_4$ for 2 h and performing electrochemical SERS in 0.1M $HClO_4$ leads to a recognizable, reversible AQDS redox wave [Fig. 8(b)] and a trend similar to the MLG/AgNP samples in the SERS spectra [Fig. 8(c)]. Upon AQDS reduction, the 1650 cm^{-1} peak disappears altogether, leaving a broad peak centered around 1600 cm^{-1}. Figure 8(d) shows the 1650 cm^{-1} peak intensity overlaid with the voltammetry.

CONCLUSIONS

We have successfully developed a SERS-active modified carbon electrode, which we think will be applicable to a variety of electrochemical studies involving adsorbed molecular species on graphitic carbon. Our strategy is similar to that used in SHINERS, where we utilize an underlying plasmonic material for enhanced Raman signal on a thin non-plasmonic layer. We used this hybrid graphene/AgNP substrate to characterize the reversible redox behavior of an adsorbed anthraquinone derivative, AQDS, on graphene in different acidic media and compared MLG and SLG. We found that

graphene had a stabilizing effect on AgNPs, helping suppress Ag oxidation and HER. Raman intensities of AQDS on bare and graphene covered substrates clearly showed the SERS effect on both. We identified a trade-off between SERS intensity and sample reproducibility: SERS on MLG/AgNP electrodes is more robust but less intense than on SLG/AgNP electrodes, albeit the latter are more difficult to produce and experiment with. Voltammetric experiments on both types of electrodes showed clear evidence of AQDS adsorption. We evaluated the SERS activity by evaluating the quinone C=O stretch at 1650 cm^{-1}, which dramatically decreased in intensity upon reduction to hydroquinone. This redox pair displayed a reversible behavior that followed changes in SERS induced electrochemically using cyclic voltammetry. Progressive drops in SERS intensity over time indicated a possible AQDS desorption and/or AgNP degradation, both likely caused by laser exposure. Future studies could more thoroughly investigate other local solution effects, such as pH, on the anthraquinone spectral signatures, as well as the role of possible photothermal effects.[35] Adjustments to substrate fabrication could include graphene transfer improvements or the use of smoother supports to obtain more homogeneous and reproducible graphene layers. This substrate should open new opportunities to study a myriad of electrode processes occurring on graphitic carbon electrodes, and we look forward to its deployment for *in situ* and *operando* studies of sensors, batteries, and electrocatalysts.

ACKNOWLEDGMENTS

This material is based upon the work supported by the National Science Foundation under CHE Grant No. 2004054. Portions of this work were carried out in part in the Materials Research Laboratory Central Research Facilities, University of Illinois. We graciously acknowledge Dr. Matthew Gole and Professor Catherine J. Murphy at the University of Illinois, Urbana-Champaign, for providing the Ag nanoparticle samples used in this study.

AUTHOR DECLARATIONS

Conflict of Interest

The authors have no conflicts to disclose.

Author Contributions

Kendrich O. Hatfield: Conceptualization (equal); Formal analysis (equal); Investigation (equal); Methodology (equal); Software (lead); Validation (lead); Visualization (lead); Writing – original draft (lead); Writing – review & editing (equal). **Seth T. Putnam**: Investigation (supporting); Validation (supporting); Writing – review & editing (supporting). **Joaquín Rodríguez-López**: Conceptualization (equal); Funding acquisition (lead); Methodology (equal); Project administration (lead); Supervision (lead); Visualization (supporting); Writing – review & editing (equal).

DATA AVAILABILITY

The data that support the findings of this study are available from the corresponding author upon reasonable request.

REFERENCES

[1] J. Wang, J. Kim, S. Choi, H. Wang, and J. Lim, "A review of carbon-supported nonprecious metals as energy-related electrocatalysts," Small Methods **4**(10), 2000621 (2020).
[2] Z. Qiao, C. Wang, Y. Zeng, J. S. Spendelow, and G. Wu, "Advanced nanocarbons for enhanced performance and durability of platinum catalysts in proton exchange membrane fuel cells," Small **17**(48), 2006805 (2021).
[3] N. Dhabarde, J. Selvaraj, A. Yuda, A. Kumar, and V. R. Subramanian, "Review of photocatalytic and photo-electrocatalytic reduction of CO_2 on carbon supported films," Int. J. Hydrogen Energy **47**(72), 30908–30936 (2022).
[4] M.-S. Balogun, Y. Luo, W. Qiu, P. Liu, and Y. Tong, "A review of carbon materials and their composites with alloy metals for sodium ion battery anodes," Carbon **98**, 162–178 (2016).
[5] T. Kim, W. Song, D.-Y. Son, L. K. Ono, and Y. Qi, "Lithium-ion batteries: Outlook on present, future, and hybridized technologies," J. Mater. Chem. A **7**, 2942 (2019).
[6] M. Maleki, G. A. El-Nagar, D. Bernsmeier, J. Schneider, and C. Roth, "Fabrication of an efficient vanadium redox flow battery electrode using a free-standing carbon-loaded electrospun nanofibrous composite," Sci. Rep. **10**, 11153 (2020).
[7] Y. Wang, L. Zhang, H. Hou, W. Xu, G. Duan, S. He, K. Liu, and S. Jiang, "Recent progress in carbon-based materials for supercapacitor electrodes: A review," J. Mater. Sci. **56**, 173–200 (2021).
[8] R. L. McCreery, "Advanced carbon electrode materials for molecular electrochemistry," Chem. Rev. **108**(7), 2646–2687 (2008).
[9] A. Ambrosi, C. K. Chua, A. Bonanni, and M. Pumera, "Electrochemistry of graphene and related materials," Chem. Rev. **114**(14), 7150–7188 (2014).
[10] K. Märker, C. Xu, and C. P. Grey, "Operando NMR of NMC811/graphite lithium-ion batteries: Structure, dynamics, and lithium metal deposition," J. Am. Chem. Soc. **142**(41), 17447–17456 (2020).
[11] M. Liu, Z.-R. Ni, H.-J. Sun, S.-H. Cao, and Z. Chen, "In situ real-time quantitative determination in electrochemical nuclear magnetic resonance spectroscopy," Sensors **22**, 282 (2022).
[12] D. A. Scherson, Y. V. Tolmachev, and I. C. Stefan, "Ultraviolet/visible spectroelectrochemistry," in *Encyclopedia of Analytical Chemistry*, edited by R. A. Meyers (John Wiley & Sons, 2006), pp. 10172–10225.
[13] J. J. A. Lozeman, P. Führer, W. Olthuis, and M. Odijk, "Spectroelectrochemistry, the future of visualizing electrode processes by hyphenating electrochemistry withe spectroscopic techniques," Analyst **145**, 2482 (2020).
[14] R. R. Jones, D. C. Hooper, L. Zhang, D. Wolverson, and V. K. Valev, "Raman techniques: Fundamentals and frontiers," Nanoscale Res. Lett. **14**, 231 (2019).
[15] T. Touzalin, S. Joiret, I. T. Lucas, and E. Maisonhaute, "Electrochemical tip-enhanced Raman spectroscopy imaging with 8 nm lateral resolution," Electrochem. Commun. **108**, 106557 (2019).
[16] Z. T. Gossage, N. B. Schorr, K. Hernández-Burgos, J. Hui, B. H. Simpson, E. C. Montoto, and J. Rodríguez-López, "Interrogating charge storage on redox active colloids via combined Raman spectroscopy and scanning electrochemical microscopy," Langmuir **33**, 9455–9463 (2017).
[17] R. Moldovan, E. Vereshchagina, K. Milenko, B.-C. Iacob, A. E. Bodoki, A. Falamas, N. Tosa, C. M. Muntean, C. Farcău, and E. Bodoki, "Review on combining surface-enhanced Raman spectroscopy and electrochemistry for analytical applications," Anal. Chim. Acta **1209**, 339250 (2022).
[18] R. Pilot, R. Signorini, C. Durante, L. Orian, M. Bhamidipati, and L. Fabris, "A review on surface-enhanced Raman scattering," Biosensors **9**, 57 (2019).
[19] J. Langer *et al.*, "Present and future of surface-enhanced Raman scattering," ACS Nano **14**, 28–117 (2020).
[20] J.-B. Wu, M.-L. Lin, X. Cong, H.-N. Liu, and P.-H. Tan, "Raman spectroscopy of graphene-based materials and its applications in related devices," Chem. Soc. Rev. **47**, 1822–1873 (2018).
[21] B. J. Kennedy, S. Spaeth, M. Dickey, and K. T. Carron, "Determination of the distance dependence and experimental effects for modified SERS substrates based on self-assembled monolayers formed using alkanethiols," J. Phys. Chem. B **103**(18), 3640–3646 (1999).

[22]X. Meng, H. Wang, N. Chen, P. Ding, H. Shi, X. Zhai, Y. Su, and Y. He, "A graphene–silver nanoparticle–silicon sandwich SERS chip for quantitative detection of molecules and capture, discrimination, and inactivation of bacteria," Anal. Chem. **90**, 5646–5653 (2018).
[23]J. F. Li, Y. F. Huang, Y. Ding, Z. L. Yang, S. B. Li, X. S. Zhou, F. R. Fan, W. Zhang, Z. Y. Zhou, D. Y. Wu *et al.*, "Shell-isolated nanoparticle-enhanced Raman spectroscopy," Nature **464**, 392–395 (2010).
[24]G. Yuan, G. Zhang, J. Chen, L. Fu, L. Xu, and F. Yang, "The electrochemical activities of anthraquinone monosulfonate adsorbed on the basal plane of reduced graphene oxide by π–π stacking interaction," J. Solid State Electrochem. **17**, 2711–2719 (2013).
[25]M. R. Gerhardt, L. Tong, R. Gómez-Bombarelli, Q. Chen, M. P. Marshak, C. J. Galvin, A. Aspuru-Guzik, R. G. Gordon, and M. J. Aziz, "Anthraquinone derivatives in aqueous flow batteries," Adv. Energy Mater. **7**, 1601488 (2017).
[26]G. Goor, W. Kunkel, and O. Weiberg, in *Ullman's Encyclopedia of Industrial Chemistry*, edited by B. Elvers, S. Hawkins, M. Ravenscroft, and G. Schulz (VCH Verlag GmbH & Co, 1989), Vol. A13, pp. 443–466.
[27]P. He, R. M. Crooks, and L. R. Faulkner, "Adsorption and electrode reactions of disulfonated anthraquinones at mercury electrodes," J. Phys. Chem. **94**, 1135–1141 (1990); J. Zhang and F. C. Anson, "Voltammetry and in-situ Fourier transform IR spectroscopy of two anthraquinone disulfonates adsorbed on graphite electrodes," J. Electroanal. Chem. **331**, 945–957 (1992).
[28]H. H. Hamzah, W. C. Chein, S. S. F. Rahiman, and S. A. Shafiee, "Investigating the effects of primary amine linkers with different carbon chain lengths on the acid dissociation constant (p*K*a) for covalently immobilized anthraquinone at the electrode surface using linear and non-linear fittings," J. Electrochem. Soc. **166**(16), H877–H887 (2019).
[29]K. O. Hatfield, M. T. Gole, N. B. Schorr, C. J. Murphy, and J. Rodríguez-López, "Surface-enhanced Raman spectroscopy-scanning electrochemical microscopy: Observation of real-time surface pH perturbations," Anal. Chem. **93**(22), 7792–7796 (2021).
[30]Y. Zeng, Z. T. Gossage, D. Sarbapalli, J. Hui, and J. Rodríguez-López, "Tracking passivation and cation flux at incipient solid-electrolyte interphases on multilayer graphene using high resolution scanning electrochemical microscopy," ChemElectroChem **9**(5), e202101445 (2022).
[31]D. Li, S. Jia, E. K. Fodjo, H. Xu, Y. Wang, and W. Deng, "*In situ* SERS and X-ray photoelectron spectroscopy studies on the pH-dependant adsorption of anthraquinone-2-carboxylic acid on silver electrode," Appl. Surf. Sci. **367**, 153–159 (2016); A. Babaei, P. A. Brooksby, A. Flood, and A. J. McQuillan, "ATR infrared spectroelectrochemistry of the reduction products of anthraquinone sulfonates in aqueous solutions," Appl. Spectrosc. **54**(4), 496–501 (2000).
[32]K. Dai, R. Huang, R. Jiang, H.-X. Ke, F. Li, S. Jin, D.-Y. Wu, and Z.-Q. Tian, "Adsorption and reduction reactions of anthraquinone derivatives on gold electrodes studies with electrochemical surface-enhanced Raman spectroscopy," J. Raman Spectrosc. **43**, 1367–1373 (2012).
[33]A. J. Bard and L. R. Faulkner, *Electrochemical Methods: Fundamentals and Applications*, 2nd ed. (John Wiley & Sons, 2001).
[34]S. W. Han, S. W. Joo, T. H. Ha, Y. Kim, and K. Kim, "Adsorption characteristics of anthraquinone-2-carboxylic acid on gold," J. Phys. Chem. B **104**, 11987–11995 (2000).
[35]N. B. Schorr, M. J. Counihan, R. Bhargava, and J. Rodríguez-López, "Impact of plasmonic photothermal effects on the reactivity of Au nanoparticle modified graphene electrodes visualized using scanning electrochemical microscopy," Anal. Chem. **92**(5), 3666–3673 (2020).